



Advanced VIRGO Interferometer: a second generation detector for Gravitational Waves observation

F. Frasconi for the VIRGO Collaboration

16th Lomonosov Conference

Moscow State University, Moscow, Russia

August 22-28, 2013

The VIRGO Collaboration



INFN - Italy

Sez. Firenze/Un. Urbino

Sez. Genova

Sez. Napoli/Un. Federico II &
Salerno

Sez. Perugia/Un. Perugia & Camerino

Sez. Pisa/Un. Pisa

Sez. Roma/Un. Sapienza

Sez. Roma2/Un. Tor Vergata

Sez. Padova/Un. Trento

EGO Group completes the
Collaboration: about 200 authors

CNRS - France

APC - Paris

ESPCI - Paris

LMA - Lyon

LAL - Orsay

LAPP - Annecy

OCA - Nice

NIKHEF - Amsterdam (NL)

RADBOUND Un. Nijmegen

POLGRAW - Warsaw (Pol)

RMKI - Budapest (Hun)

The Interferometer at EGO site



Advanced VIRGO



August 24, 2013

F. Frasconi / INFN Pisa

3

Gravitational Waves

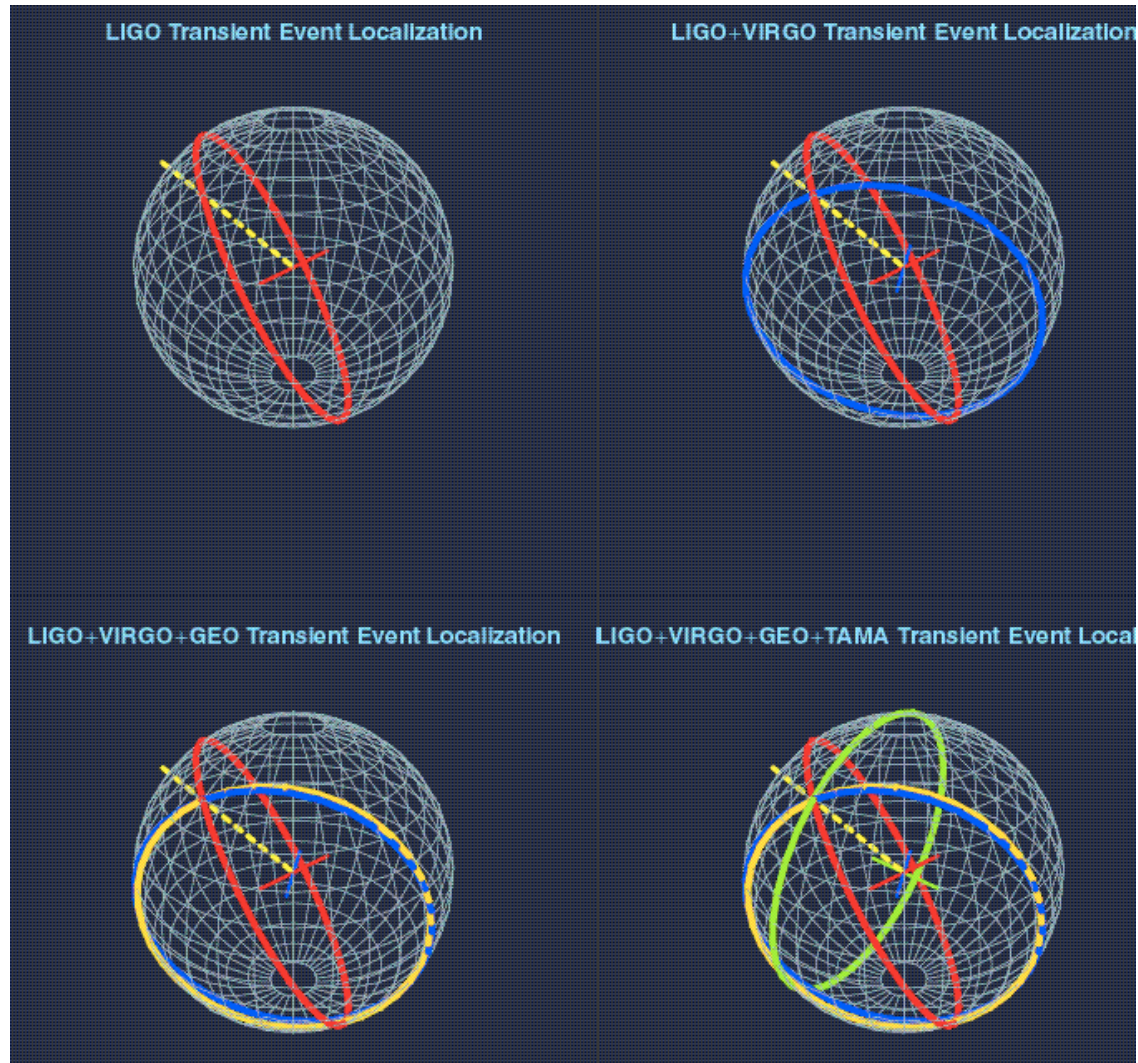


- According to the Einstein's theory of General Relativity (1915), **Gravitational Waves (GW)** are perturbations of the "space-time" metric traveling in the Universe at the speed of light;
- They are expected to be emitted by astrophysical processes in which accelerated coherent motions of large masses take place (supernova explosions, pulsars, etc.);
- The aim of ground based interferometric detectors (ITF) is the direct observation of *GW* together with the possibility to localize their source in the sky (detectors network).

Importance of a detectors Network



- False alarm rejection requires coincidence
- Triangulation allows to pinpoint the source
- The Network allows to deconvolve detector response and signal wave form -> measurement of the signal parameters
- Longer observation time better sky coverage



Network: ITFs of the 1st Generation



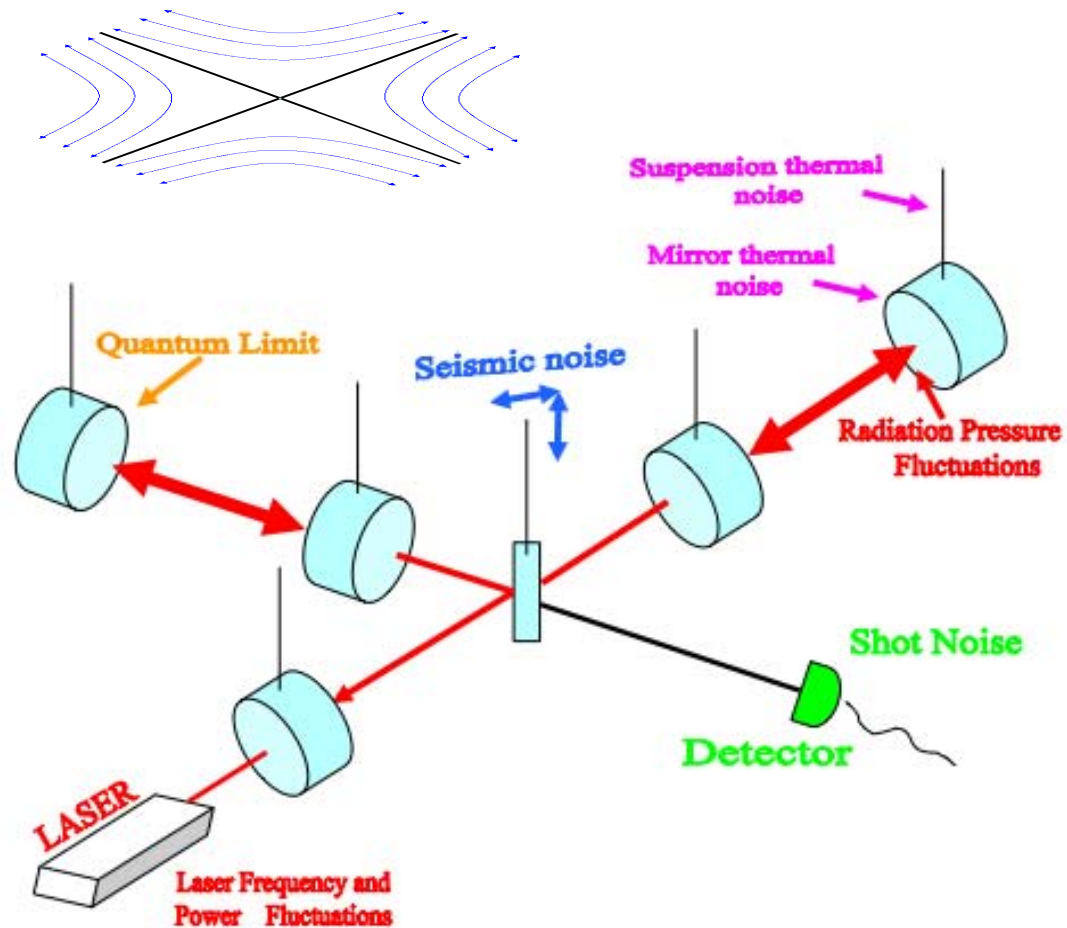
The broad band GW interferometers



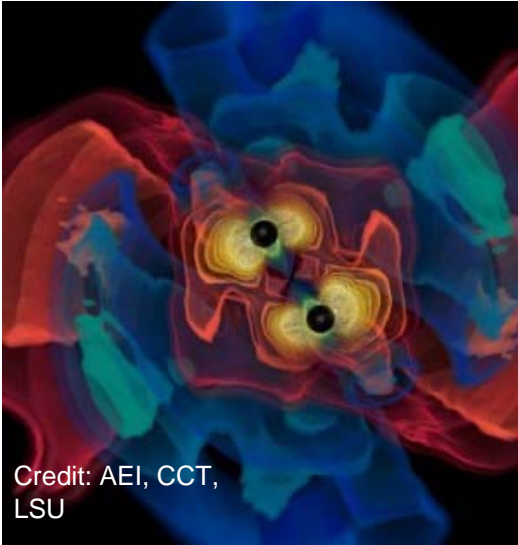
- The detector is sensitive to h the Gravitational Wave strain amplitude (a GW impinging on the plane of a suspended interferometer stretches one arm compressing the other one alternatively)

- The detector sensitivity is expressed in terms of the amplitude spectral density of the detector noise referred to its input

$$H(f) \quad [(\text{Hz})^{-1/2}]$$



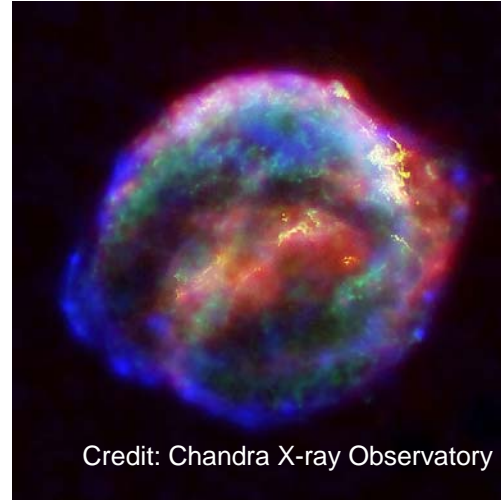
Sources of GW



Credit: AEI, CCT, LSU

Coalescing Binary Systems

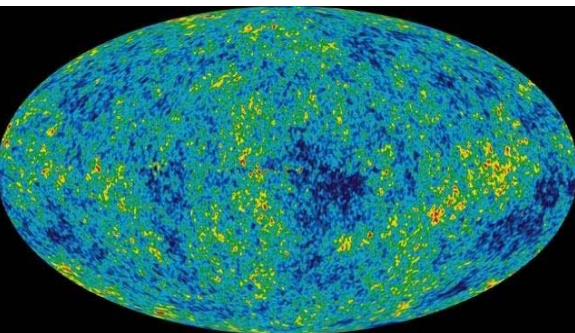
- Neutron stars, low mass black holes, and NS/BS systems



Credit: Chandra X-ray Observatory

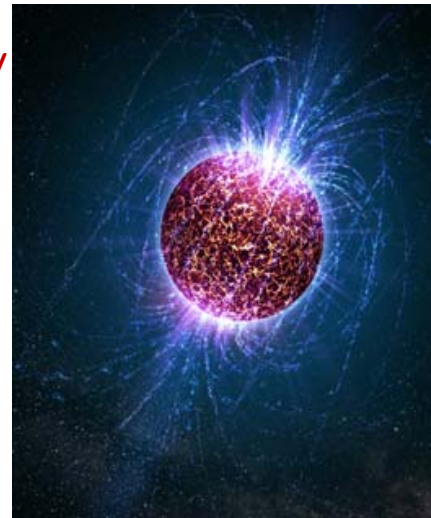
'Bursts'

- galactic asymmetric core collapse supernovae
- cosmic strings
- ???



Cosmic GW background

- Stochastic, incoherent background
- unlikely to detect, but can bound in the 10-10000 Hz range



Continuous Sources

- Spinning neutron stars
- probe crustal deformations, 'quarkiness'

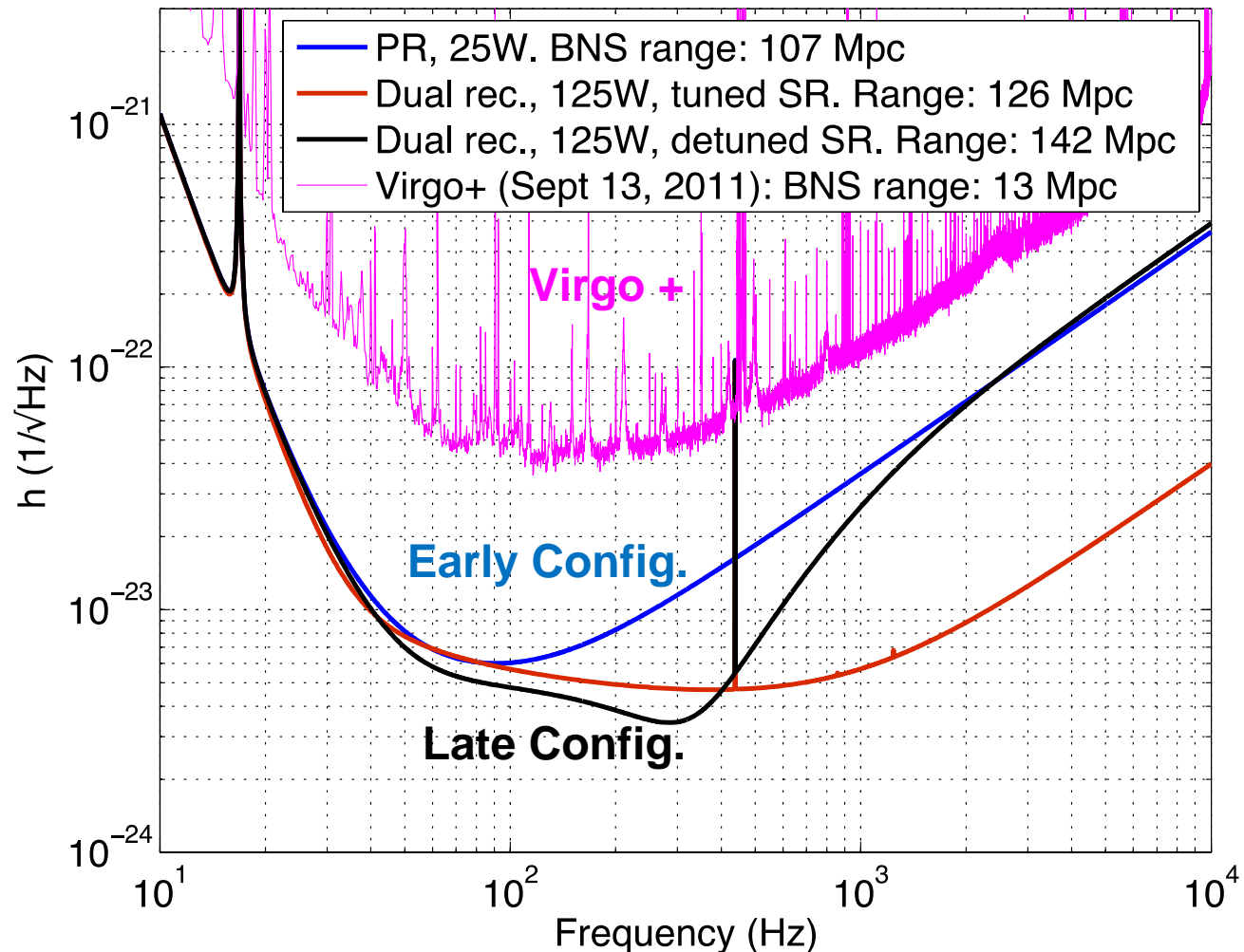
Advanced VIRGO Interferometer



- Advanced VIRGO: upgrade of the VIRGO Interferometer
- Michelson Interferometer with two Fabry-Perot cavities along the arms 3 km long each one



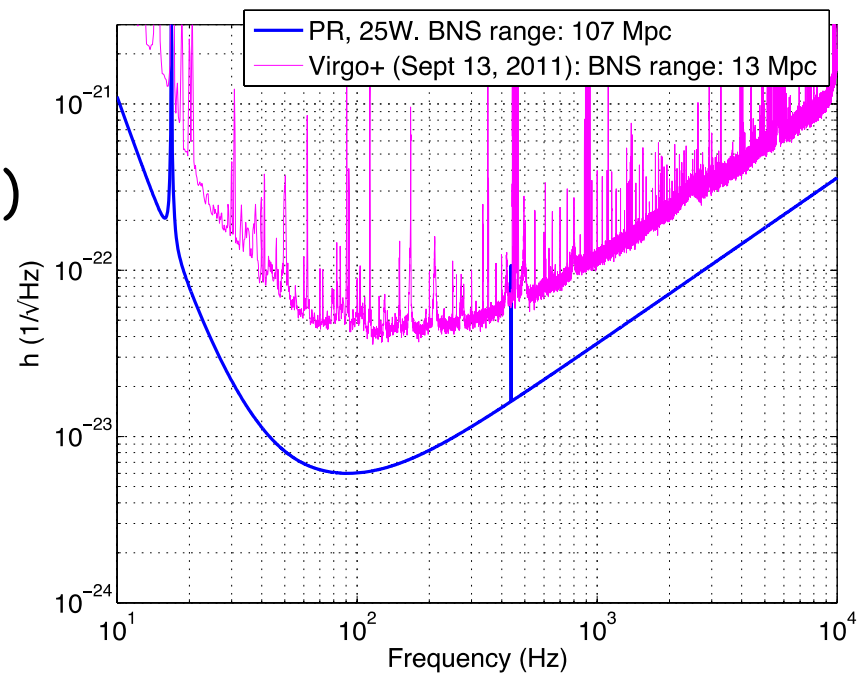
Evolution of ITF sensitivity



Toward AdV operation



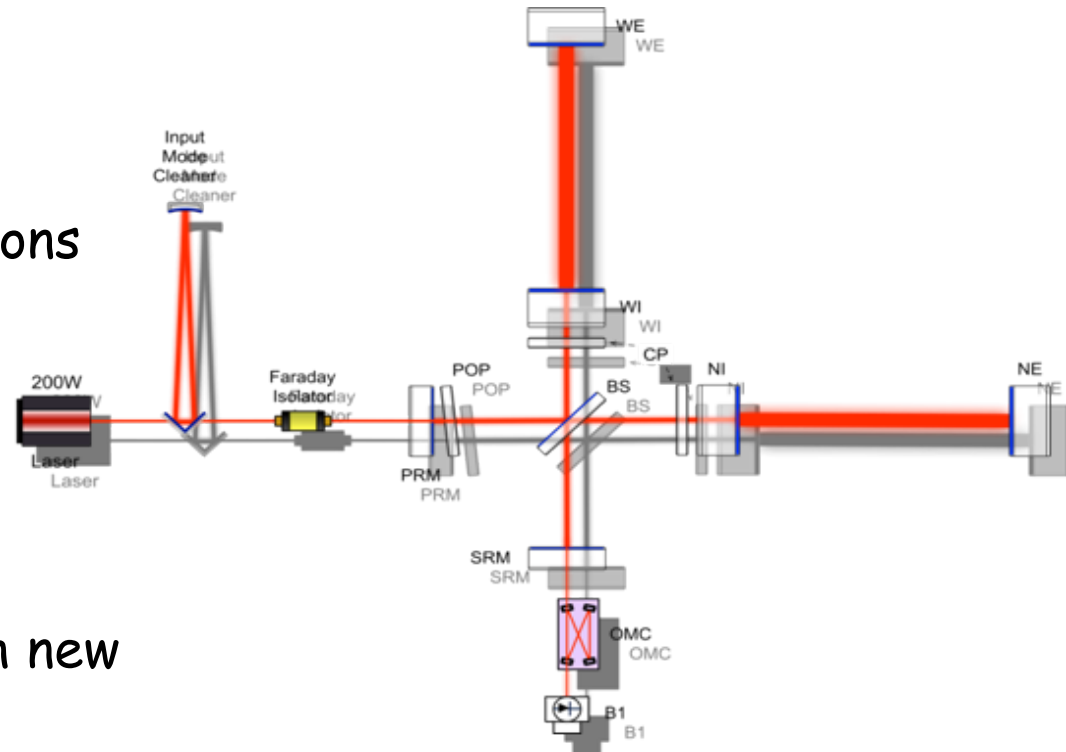
- Start in 2015 putting in operation the ITF with a simplified configuration, similar to VIRGO+ : likely to reduce the commissioning time
 - without Signal recycling
 - VIRGO+ laser up to 60 W
 - low power (reduced risks with thermal effects and high power laser)
- Target BNS inspiral range: > 100 Mpc



Detector Design



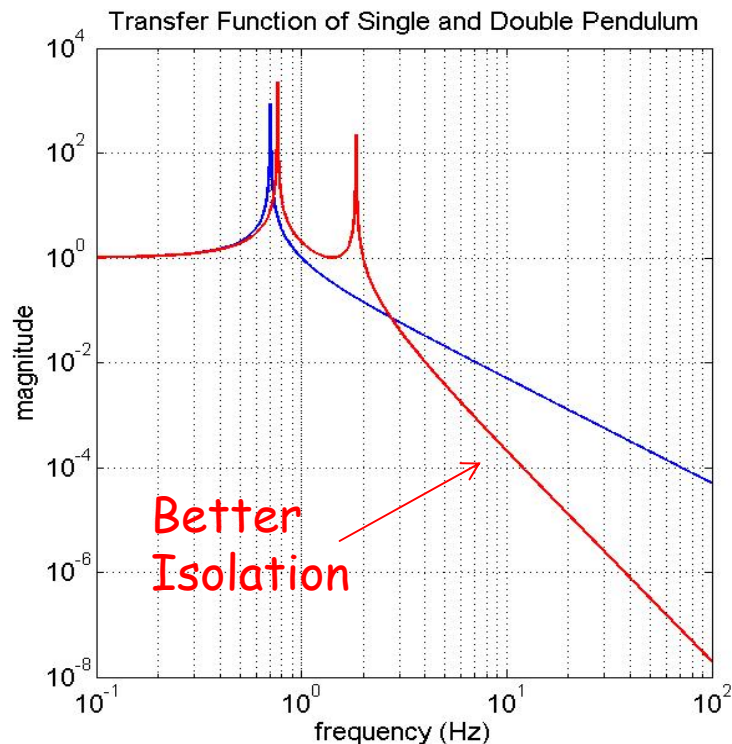
- Main changes with respect to VIRGO:
 - larger beam
 - heavier mirrors
 - higher quality optics
 - thermal control of aberrations
 - 200W fiber laser
 - Signal Recycling
- Vibration isolation by VIRGO Superattenuators:
 - performance compliant with new requirements
 - wide experience with commissioning at low frequency



Seismic Noise



- Seismic noise limits sensitivity of ground based detectors at low frequencies - "seismic wall"
- Typical seismic noise at EGO site at 10 Hz is $\sim \text{few} \times 10^{-10} \text{ m}/\sqrt{\text{Hz}}$
 - many orders of magnitude above target noise level
- Solution - multiple stages of isolation system
- Isolation required in vertical direction as well as horizontal due to cross-coupling

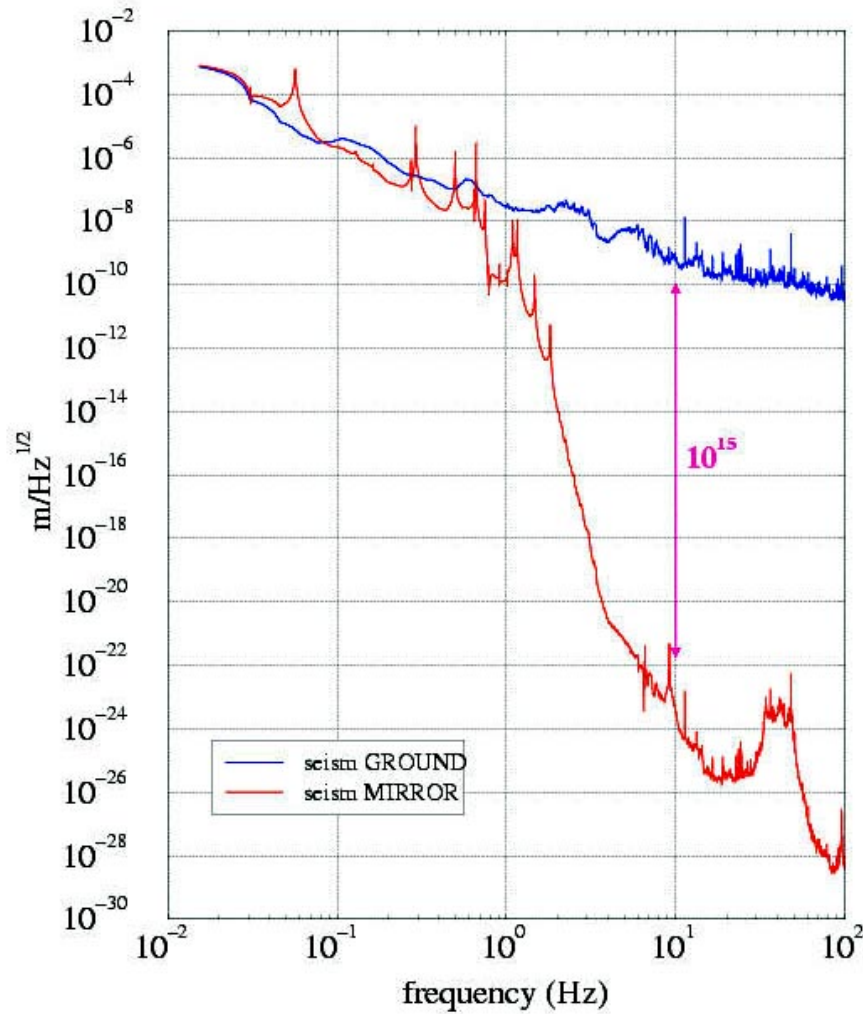


Advantages of a **double** over **single** pendulum, same overall length

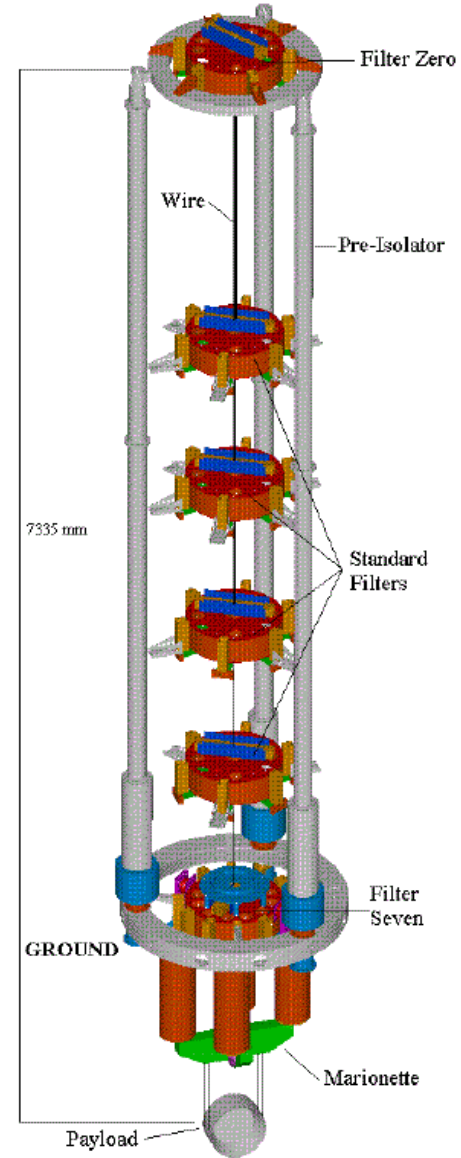
Mirror Suspensions



• r
i
f
c
v
F
t
c



re
le
e

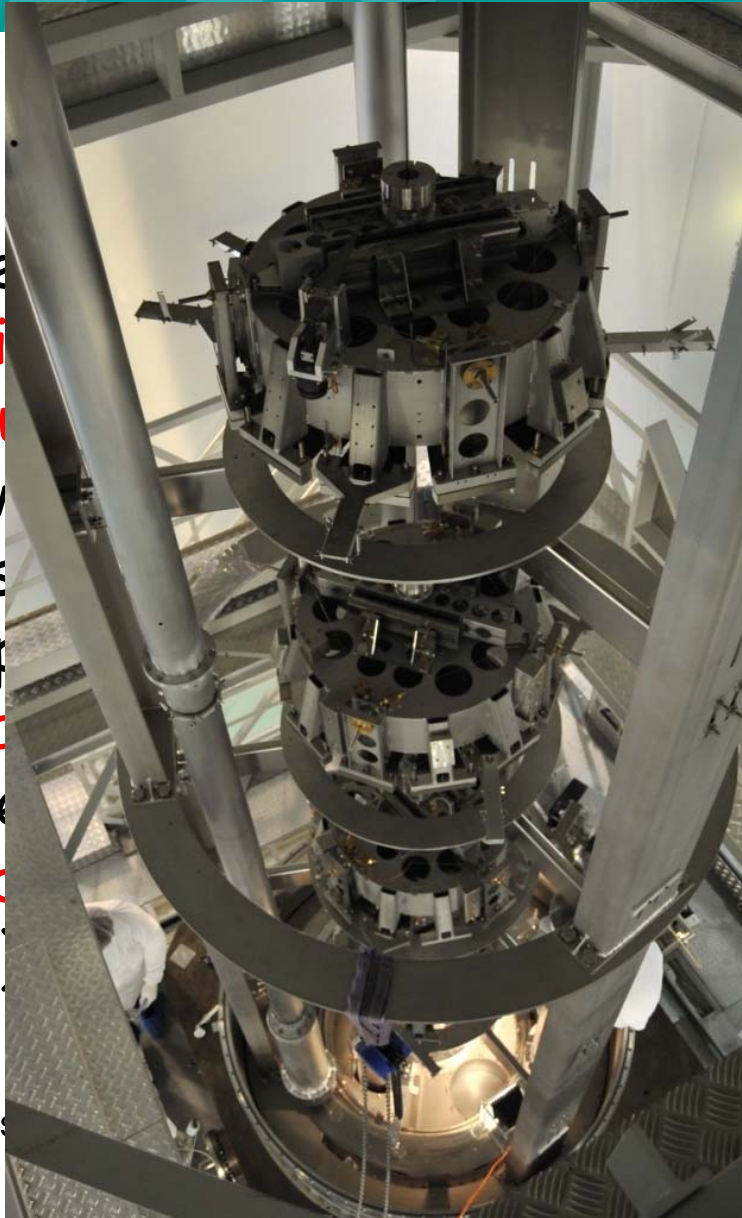


↓ Pisa

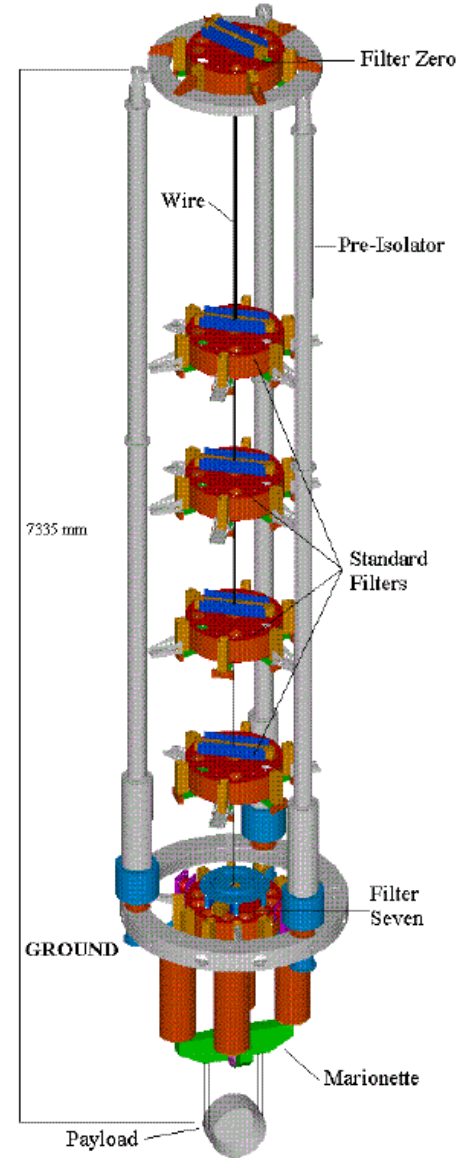
The SA chain



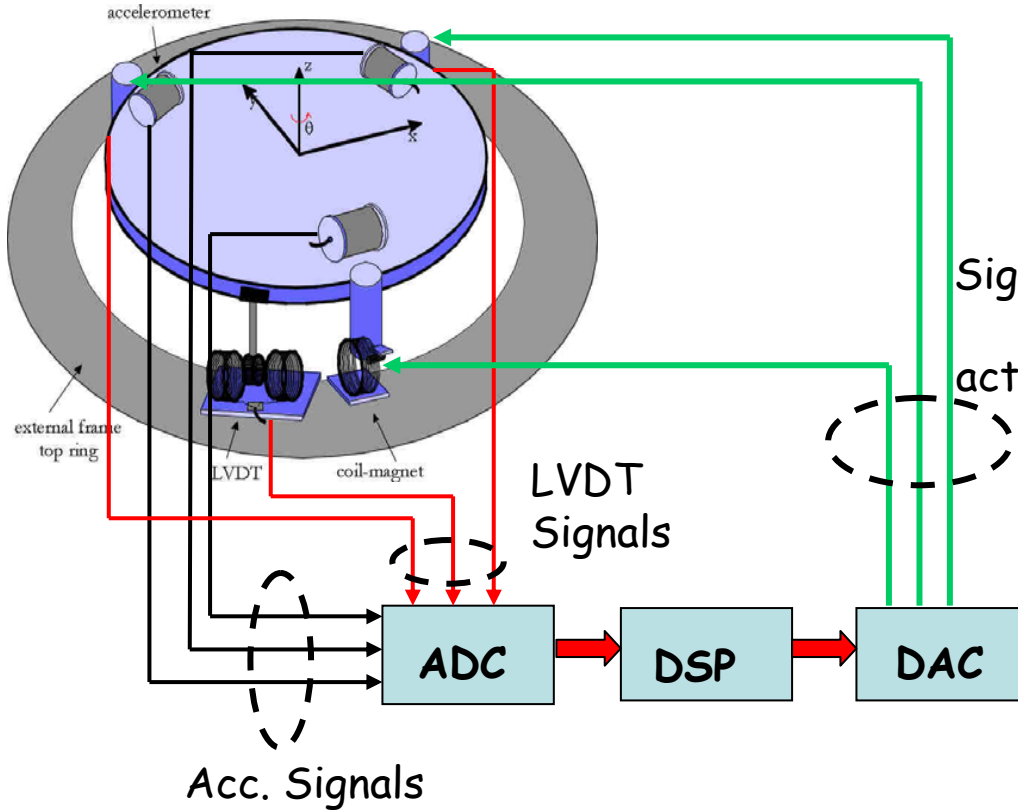
- The pre-isolator filters frequencies above 100 Hz to allow the suspension to oscillate at the seismic frequencies.
- It provides a hierarchical suspension and damping system with a bandwidth of ~200 Hz.



is a
 ed to
 ol of
 .
 rain
 ~200



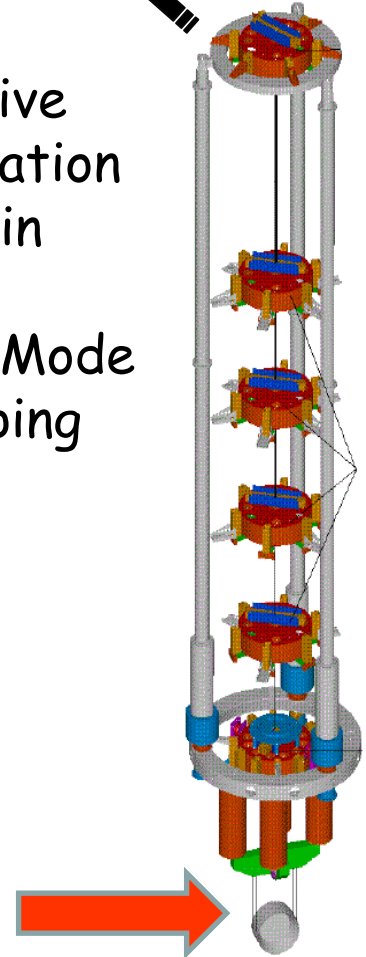
Main features of SA



Passive
attenuation
chain
+
Active Mode
Damping

Standard
Filters

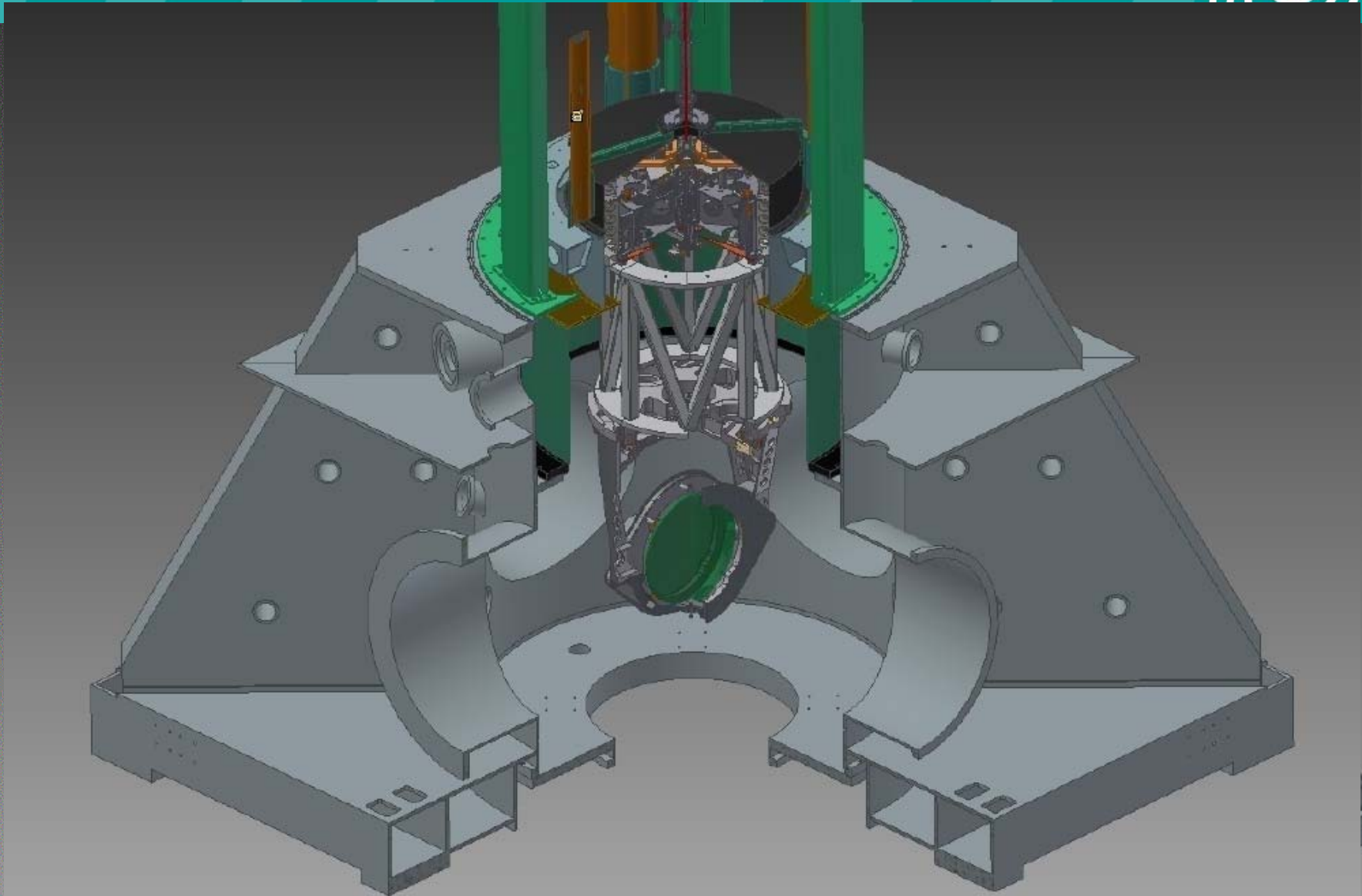
Residual swing at Payload level
LONGITUDINAL: about 100 nm pp
ANGLES: fractions of μ rad pp



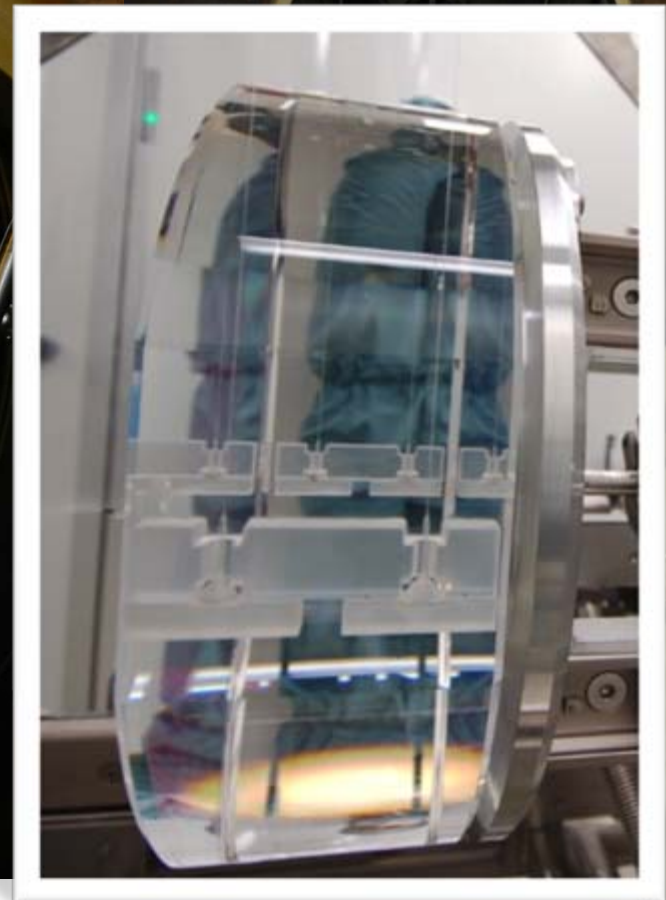
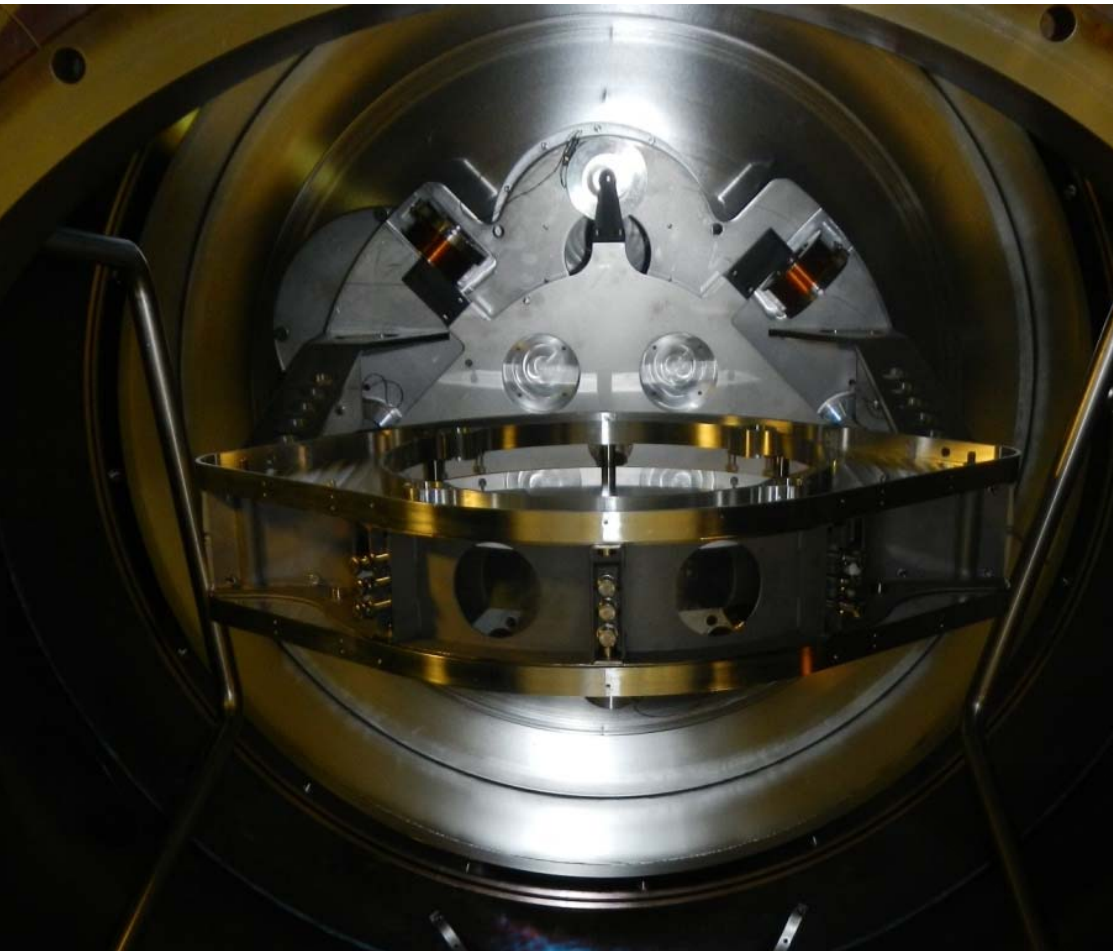


- Different **spatial distribution** of the mechanical filters along the suspension chain (optimization of seismic noise filtering in accordance with a new geometry of the Intermediate Vacuum Chamber)
- Re-tuning of mechanical filters in accordance with the load to be supported (heavier mirrors + new TCS + baffles)
- Re-design and construction of the last mechanical filter (**Filter7**) in accordance with the new Payloads geometry (presence of large baffle for diffused light mitigation)
- Construction of **new control electronics**:
 - analog and digital parts embedded in a single board
 - about 100 channels per SA

Mirror Suspension Comparison



AdV Payloads



August 24, 2013

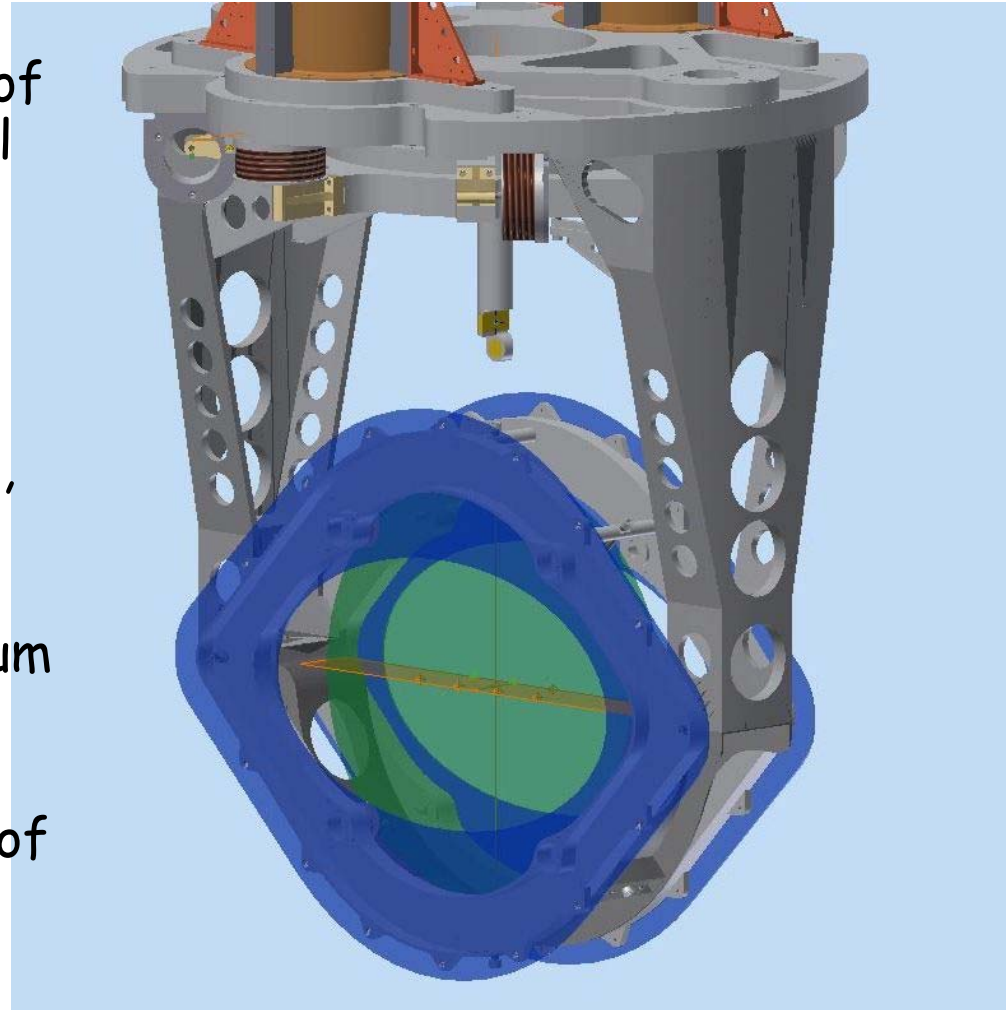
F. Frasconi / INFN Pisa

19

Stray light mitigation



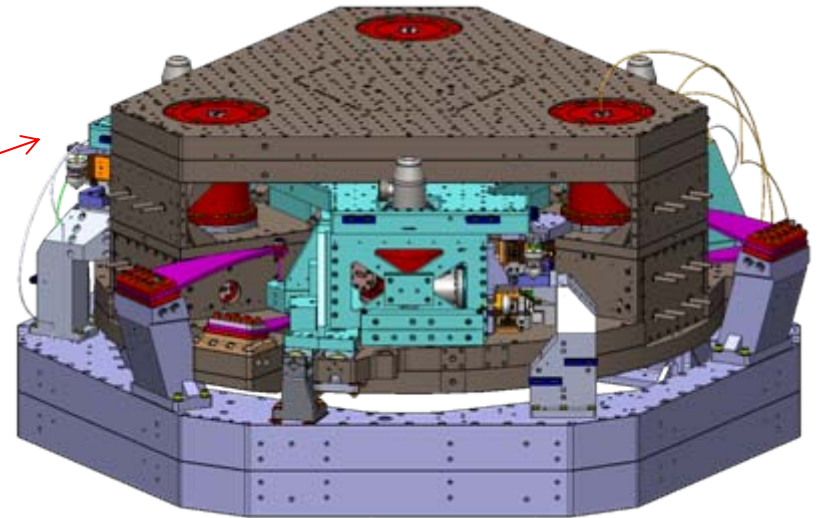
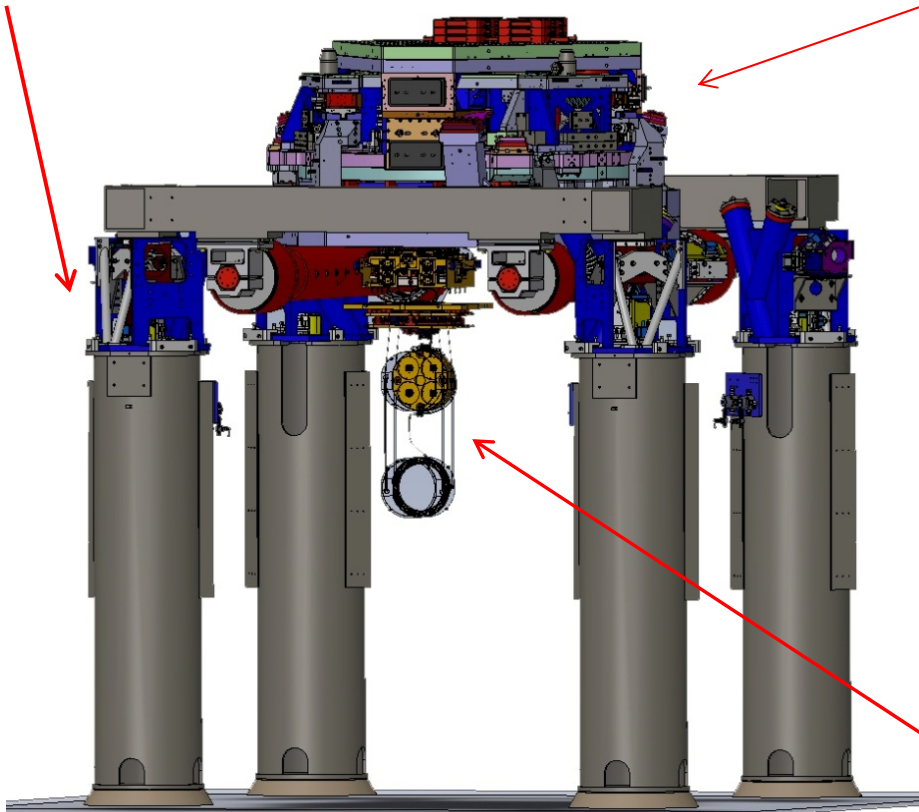
- Lesson from 1st generation detector: scattered light is one of the major risks towards the final sensitivity goal
- A big effort has been done to mitigate it:
 - better optics quality
 - baffles to shield mirrors, pipes, vacuum chamber exposed to scattered light
 - photodiodes suspended in vacuum to isolate them from seismic/acoustic noise
 - if needed, control the position of the benches with respect to the ITF



aLIGO Seismic Isolation



Hydraulic external pre-isolator
(HEPI - one stage of isolation; low
frequency positioning)



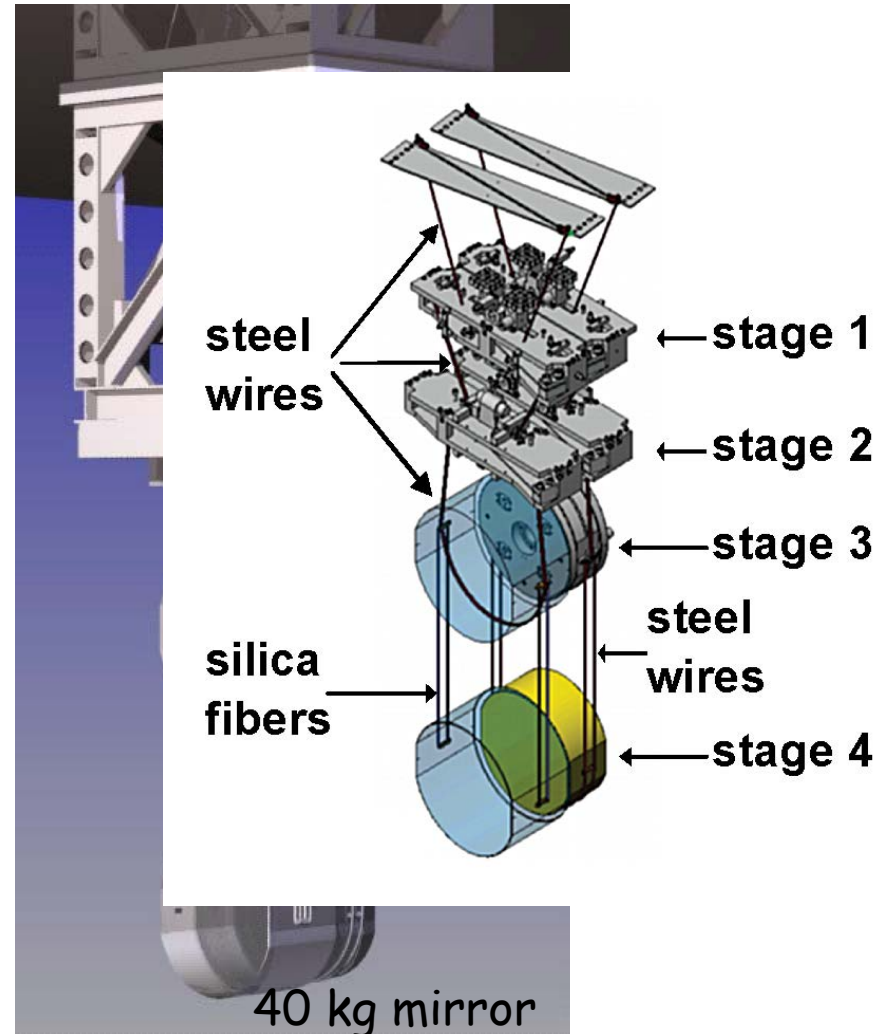
Active isolation platform (two stages
of isolation - isolate above ~ 0.2 Hz)

Quadruple pendulum (four stages
of isolation) with monolithic silica
fiber last stage

aLIGO Seismic Isolation (cont.)



- Thermal noise reduction: use monolithic fused silica suspension as final stage
- Seismic isolation: use quadruple pendulum + 3 stages of maraging steel blades for vertical isolation
- Control noise minimizing: apply damping at top mass (for 6 degrees of freedom) + use quiet reaction pendulum for global control actuation
 - coil/magnet actuation at top 3 stages
 - electrostatic drive at test mass
- Design is developed from the GEO 600 triple pendulums which have been in operation for more than 10 years



KAGRA: underground detector



- Underground ITF located in the Kamioka mine (Japan) with 3 km orthogonal arms:
 - reduced seismic noise (about a factor 50 @ 10 Hz) and gravity noise
 - simplified seismic isolation system
- Second phase: cryogenic cooling of test masses:
 - reduced thermal noise

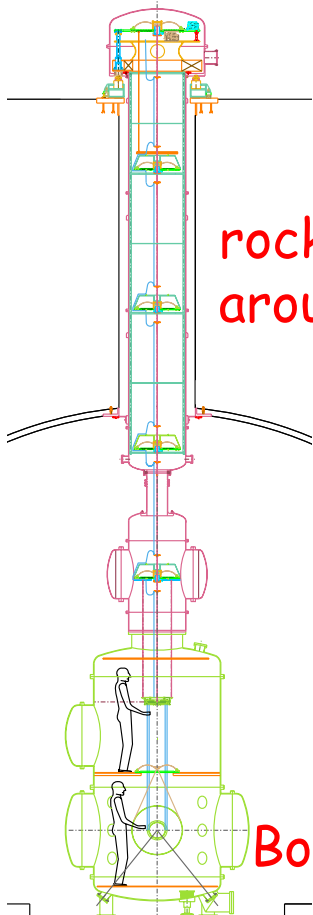
KAGRA



KAGRA Vibration Isolation



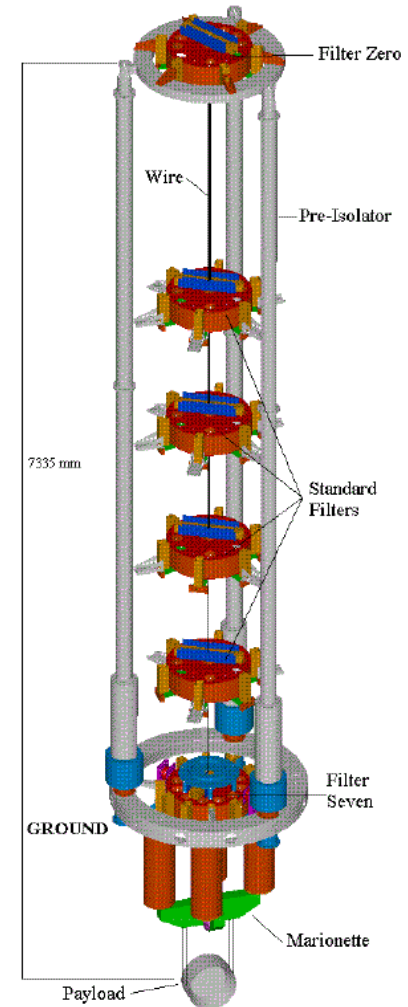
Top Tunnel



rocks all around

Bottom Tunnel

- KAGRA SAS (Seismic Attenuation System) is mounted between two tunnels:
 - a simplified and improved version of the VIRGO Superattenuator
- Good filtering performance
- New Features:
 - Geometric anti-spring (**GAS**) filters replaces Magnetic anti-spring (**MAS**) filters
 - **Magnetic damping** stage
 - **Compact pre-isolator** stage (IP)



KAGRA SAS schematic view



Cryostat in the F-P cavities: to be cooled down at cryogenic temperatures in a second phase

Pre-isolator

Filter Chain

Payload

Top Filter (Filter 0)

Inverted Pendulum

Geometric anti-spring (GAS) chain (Filter 1-3)

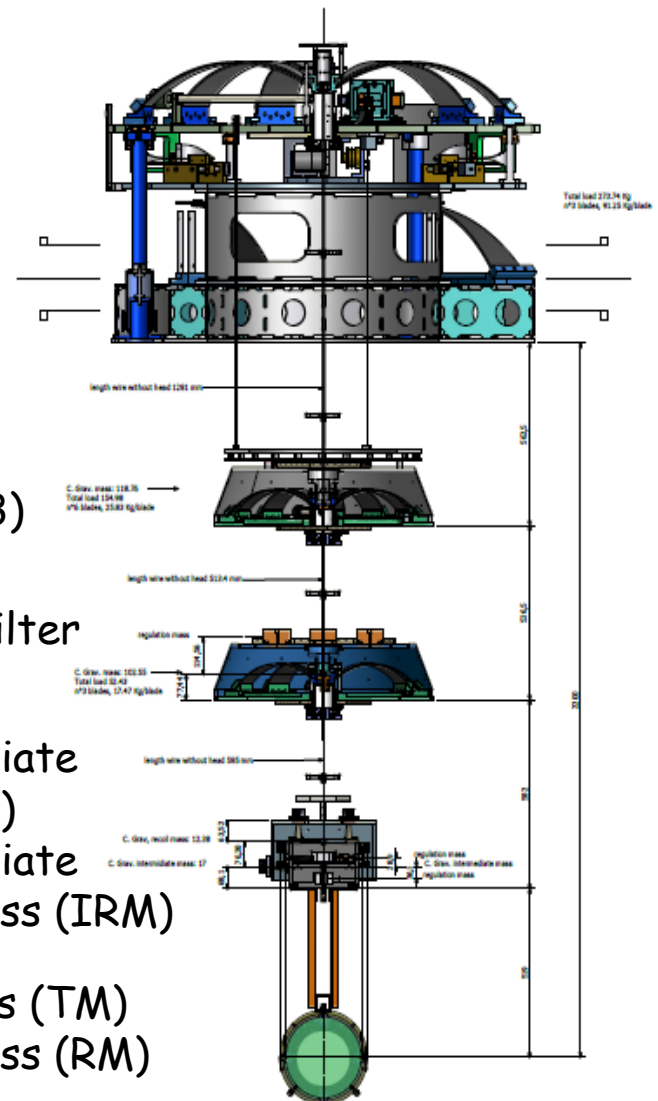
Bottom Filter (BF)

Intermediate Mass (IM)

Intermediate Recoil Mass (IRM)

Test Mass (TM)

Recoil Mass (RM)



Network: ITFs of the 2nd Generation



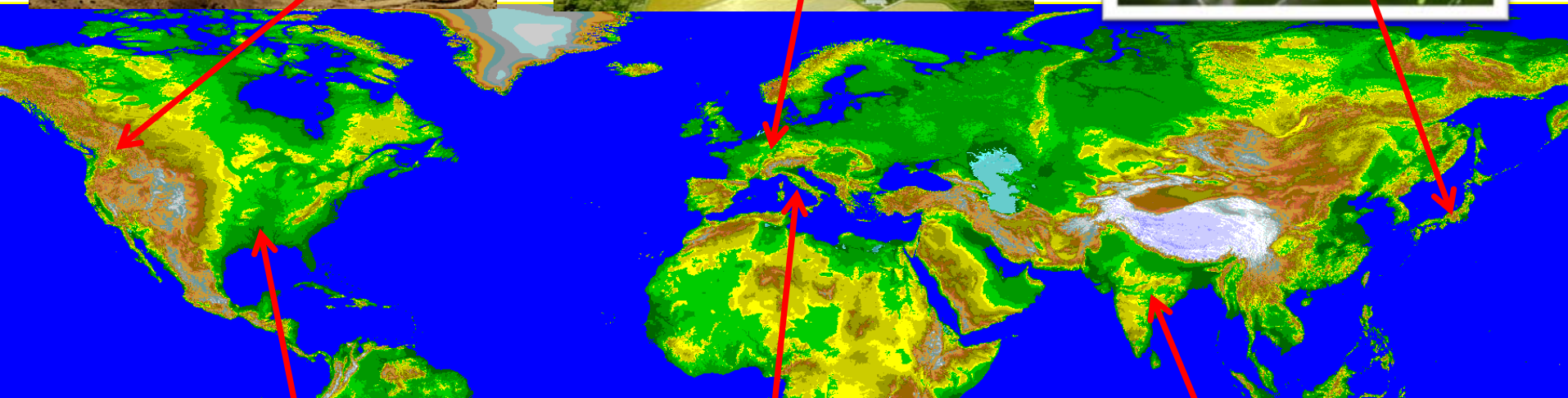
aLIGO-HA



GEO-HF



KAGRA



aLIGO-LI



Advanced VIRGO



indigo

aLIGO-India

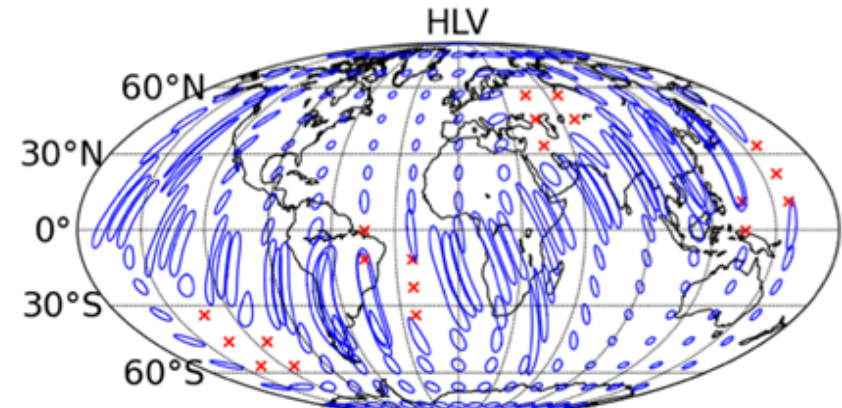
2nd Generation Network



Prospects for Localization of Gravitational Wave Transients by the Advanced LIGO and Advanced Virgo Observatories

Source localization in the sky

J. Aasi¹, J. Abadie¹, B. P. Abbott¹, R. Abbott¹, T. D. Abbott², M. Abernathy³, T. Accadia⁴, F. Acernese^{5ac}, C. Adams⁶, T. Adams⁷, P. Addresso⁸, R. X. Adhikari¹, C. Affeldt^{9,10}, M. Agathos^{11a}, O. D. Aguiar¹², P. Ajith¹, B. Allen^{9,13,10}, A. Allocca^{14ac}, E. Amador Ceron¹³, D. Amariutei¹⁵, S. B. Anderson¹, W. G. Anderson¹³, K. Arai¹, M. C. Araya¹, C. Arceneaux¹⁶, S. Ast^{9,10}, S. M. Aston⁶, P. Astone^{17a}, D. Atkinson¹⁸, P. Aufmuth^{10,9}, C. Aulbert^{9,10}, L. Austin¹, B. E. Aylott¹, P. Baker²¹, G. Ballardin²², S. Ballmer²³, Y. Bao¹⁵, J. C. Barayoga¹, D. Barker¹⁸, F. Bar L. Barsotti²⁴, M. Barsuglia²⁵, M. A. Barton¹⁸, I. Bartos²⁶, R. Bassiri^{3,27}, M. Bastarrika J. Batch¹⁸, J. Bauchrowitz^{9,10}, Th. S. Bauer^{11a}, M. Bebrone⁴, B. Behnke²⁰, M. Bejger²⁸, A. S. Bell³, C. Bell³, G. Bergmann^{9,10}, J. M. Berliner¹⁸, A. Bertolini^{9,10}, J. Betzwieser⁶, P. T. Beysersdorff²⁹, T. Bhadrade²⁷, I. A. Bilenko³⁰, G. Billingsley¹, J. Birch⁶, S. Biscani², M. A. Bizouard^{31a}, E. Black¹, J. K. Blackburn¹, L. Blackburn³², D. Blair³³, B. Bland²¹, O. Bock^{9,10}, T. P. Bodiya²⁴, C. Bogan^{9,10}, C. Bond¹⁹, F. Bondu^{34b}, L. Bonelli^{14ab}, R. R. Bork¹, M. Born^{9,10}, V. Boschi^{14a}, S. Bose³⁶, L. Bosi^{37a}, B. Bouhou²⁵, J. Bowers², C. P. R. Brady¹³, V. B. Braginsky³⁰, M. Branchesi^{38ab}, J. E. Brau³⁹, J. Breyer^{9,10}, T. D. O. Bridges⁶, A. Brillet^{34a}, M. Brinkmann^{9,10}, V. Brisson^{31a}, M. Britzger^{9,10}, A. D. A. Brown²³, D. D. Brown¹⁹, F. Brueckner¹⁹, K. Buckland¹, T. Bulik^{28b}, H. J. E. A. Buonanno⁴¹, J. Burguet-Castell⁴², D. Buskulic⁴, C. Buy²⁵, R. L. Byer²⁷, L. Ca G. Cagnoli^{35,44}, E. Calloni^{5ab}, J. B. Camp³², P. Campsie³, K. Cannon⁴⁵, B. Canuel², C. D. Capano⁴¹, F. Carbognani²², L. Carbone¹⁹, S. Caride⁴⁷, A. D. Castiglia⁴⁸, S. M. Cavaglia¹⁶, F. Cavalier^{31a}, R. Cavalieri²², G. Cella^{14a}, C. Cepeda¹, E. Cesarini^{49a}, T. S. Chao¹⁰¹, P. Charlton⁵⁰, E. Chassande-Mottin²⁵, X. Chen³³, Y. Chen⁵¹, A. Chincarini⁵², H. S. Cho⁵³, J. Chow⁵⁴, N. Christensen⁵⁵, Q. Chu³³, S. S. Y. Chua⁵⁴, C. T. Y. Chung¹, F. Clara¹⁸, D. E. Clark²⁷, J. A. Clark⁴³, F. Cleva^{34a}, E. Coccia^{49ab}, P.-F. Cohadon⁴⁰, C. A. Colla^{17ab}, M. Colombini^{17b}, M. Constanicio Jr.¹², A. Conte^{17ab}, D. Cook¹⁸, T. R. Corbit



Epoch	Estimated Run Duration	$E_{GW} = 10^{-2} M_{\odot} c^2$ Burst Range (Mpc)		BNS Range (Mpc)		Number of BNS Detections	% BNS Localized within	
		LIGO	Virgo	LIGO	Virgo		5 deg ²	20 deg ²
2015	3 months	40 – 60	–	40 – 80	–	0.0004 – 3	–	–
2016–17	6 months	60 – 75	20 – 40	80 – 120	20 – 60	0.006 – 20	2	5 – 12
2017–18	9 months	75 – 90	40 – 50	120 – 170	60 – 85	0.04 – 100	1 – 2	10 – 12
2019+	(per year)	105	40 – 80	200	65 – 130	0.2 – 200	3 – 8	8 – 28
2022+ (India)	(per year)	105	80	200	130	0.4 – 400	17	48

Conclusions



- Still waiting for the first detection ...
- Fundamental experience acquired with the 1st generation of ground based ITF:
 - wide experience collected in operating sophisticated detectors
 - important results obtained with collected data
- The construction of the Advanced Detectors (target sensitivity **10 times** better) is in progress:
 - end of AdV installation in the fall of 2015
- They will increase of a **factor 10^3 the observable volume** of the Universe opening the phase of the GW astronomy